First steps with HLLMHD and PP reconstruction

by *O. Steiner, P. Rajaguru,* and *G. Vigeesh*

We have carried out some real application runs with the CO5BOLD version of April 28, 2011, which newly allows for the combination of the HLL solver for MHD (HLLMHD) with a piecewise parabolic (PP) reconstruction. Tests consisted of box-in-the-Sun simulations with $n1 \times n2 \times n3 = 120 \times 120 \times 120$ grid cells. The size of the box is 4.8 Mm $\times$ 4.8 Mm $\times$ 2.8 Mm. The $\tau = 1$ level is at a height of about 1.5 Mm from the bottom. The grid cells have a horizontal width of 40 km and a vertical extent varying from 50 km in the bottom part of the convection zone to 20 km in the top part of the convection zone, the photosphere and the chromosphere. The initial model consists of relaxed convection as computed with HLLMHD and Van Leer reconstruction. The initial magnetic field is homogeneous and vertical with a strength of 50 G. Table 1 shows a compilation of the models we were running. Additionally we have models from previous runs for comparison.

job	solver	reconstr.	N_ordCT	$v_{\mathrm{art.}}$	B_{init}	initial model	t_{end}
job_pp_hancock	HLLMHD	PP	1	0.0	$B_z = 50$ G	rmhd120x120x120_v50	540 s
Nord_ConsTrans	HLLMHD	PP	2	0.0	$B_z = 50$ G	rmhd120x120x120_v50	540 s
job_ifort	HLLMHD	PP	1	0.0	$B_z = 50$ G	rmhd120x120x120_v50	540 s
job_pp_hancock_nu0p5	HLLMHD	PP	1	0.5	$B_z = 50$ G	rmhd120x120x120_v50	540 s
job_vanleer_hancock	HLLMHD	VanLeer	1	0.0	$B_z = 50$ G	rmhd120x120x120_v50	540 s
job_pp_eint	HLLMHD	PP	2	0.0	$B_z = 50$ G	rmhd120x120x120_v50	540 s
job3dB0	HLLMHD	PP	2	0.0	$B_z = 0$ G	rmhd240x240x240	1200 s
job3dRoe	Roe	VanLeer	—	0.0	—	rhd120x120x120	1200 s

Table 1: Models. For job_pp_eint beta_inv was set 0.0. In all other cases beta_inv=10.0

Intensity

Figure 1 shows the bolometric radiative intensity through the top boundary of the box. The model was advanced in time for 540 s. The top panel shows the intensity when advanced with the HLL and the Van Leer reconstruction scheme. The bottom panel shows the intensity when the model was advanced with HLL and PP reconstruction.

While the correspondence of individual granules can still be identified in both panels, the granules in the bottom panel (HLL PP) show much more structure than those in the top panel, which look more diffuse and washed out. In fact, we will see later that in the pure hydrodynamic case, the solution obtained with HLL PP comes close to the solution obtained with the Roe solver.

Figure 2 shows the vertical magnetic field strength at a depth of $\langle\tau\rangle = 1$. We see that the brightenings in the intergranular lanes correspond to magnetic flux concentrations. This effect (the hot wall effect) is much more pronounced in the simulation with HLL PP than in the simulation with HLL Van Leer. Note for example the bright point in the vertex near the upper right corner of the PP simulation, which corresponds to a flux concentration in the map of B_z, is absent in the Van Leer simulation.

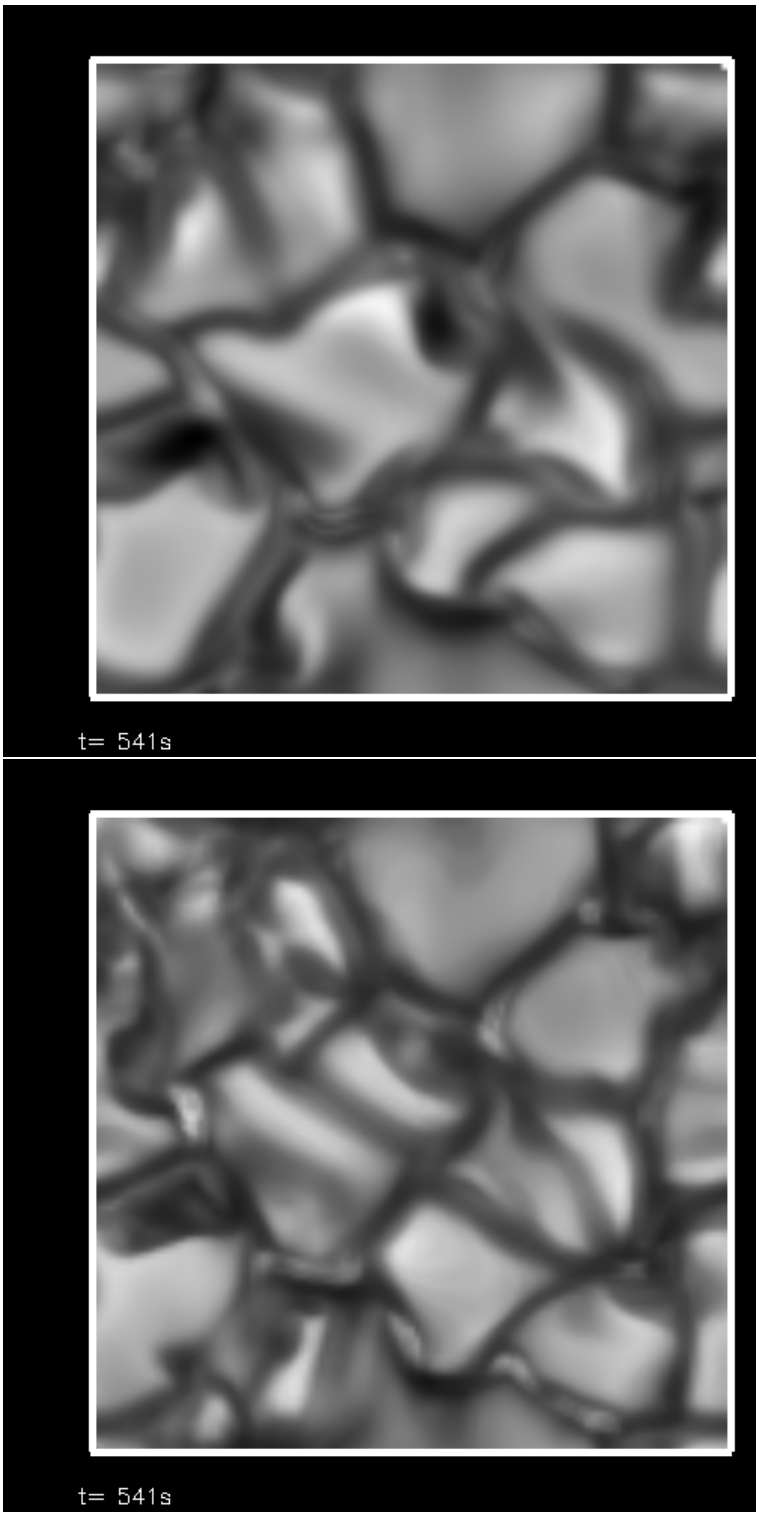

Figure 1: Bolometric intensity from a model advanced for 540 s with HLLMHD and Van Leer reconstruction (top panel) and HLLMHD and PP reconstruction (bottom panel)

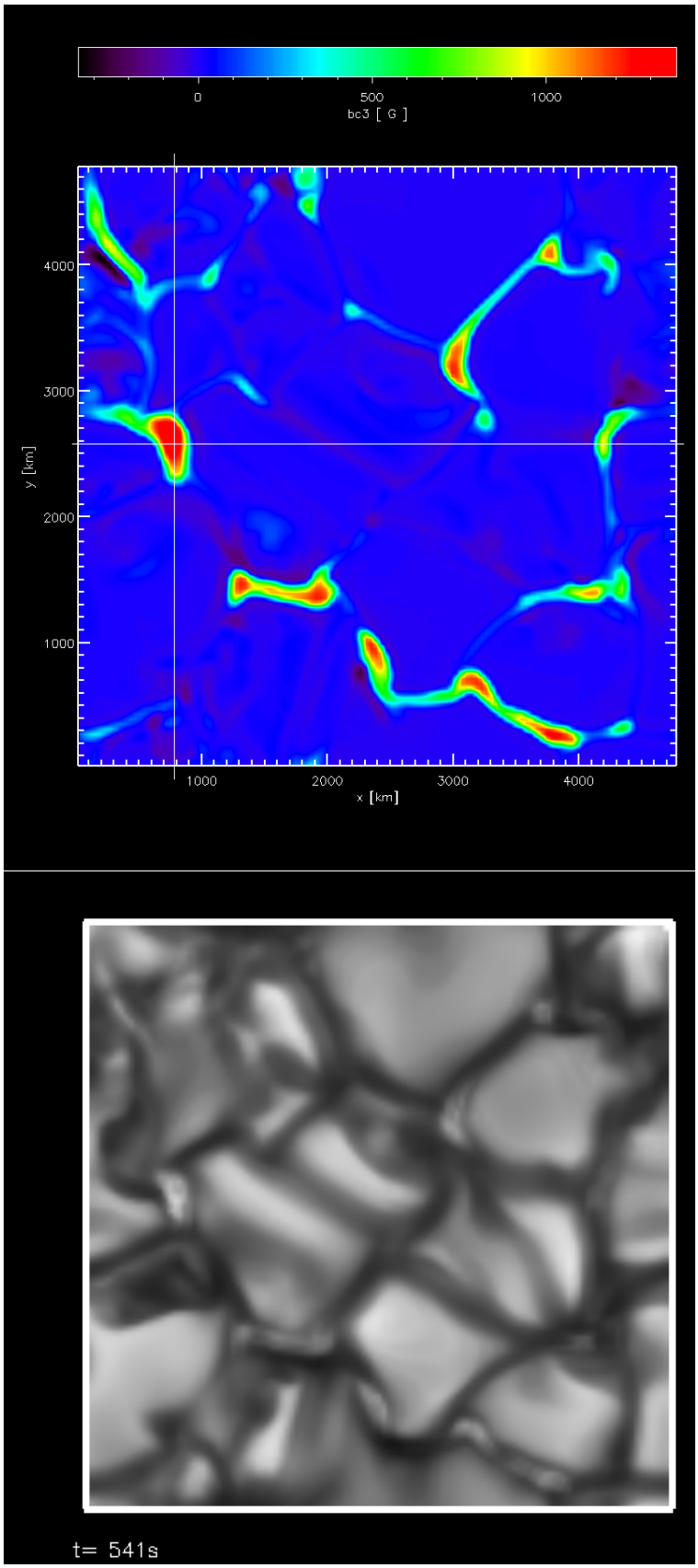

Figure 2: Magnetic flux density in the vertical direction (top panel) and bolometric intensity (bottom panel) from a simulation with HLLMHD and PP reconstruction after 540 s.

Temperature

Figure 3 shows the temperature at a level of $\langle\tau\rangle = 1$ for the simulation with HLL and Van Leer (top panel) and the simulation with HLL and PP (bottom panel). Here, the differences are less pronounced except that the numerical grid is more visible in the bottom panel.

This situation changes drastically when considering the temperature at a hight level of 1200 km above $\langle\tau\rangle = 1$. Figure 4 shows, in the top panel, $T(z = 1200\,\mathrm{km})$ from the HLL Van Leer simulation and in the bottom the same quantity from the HLL PP simulation. Because the velocities at these heights are much larger than at $\langle\tau\rangle = 1$, the time scale is much shorter and therefore the details of the two temperature maps do not correspond to each other anymore—the two solutions start to diverge. The sharp edges in the temperature maps are caused by shock fronts. The solution from the HLL PP simulation is not smooth anymore and shows strong wiggles and sawteeth.

In order to smooth this shaky solution, we first ran a simulation with PP reconstruction and setting the parameter `c_visartificial=1.0` (before, it was set to zero, while `c_vissmagorinsky=0.5` in all cases). Figure 5 shows the corresponding solution. It does not substantially differ from the original solution in Figure 4 (bottom panel). In fact it tends to be worse in the sense that it produces some very low temperature pixels with temperatures close to 2000 K.

Next we tried setting the parameter `N_orderConstrainedTransport=2` . Previously, this parameter was not set, meaning that the default value 1 was used. Figure 6 shows the corresponding solution. Again, it does not substantially differ from the original solution in Figure 4 (bottom panel). Thus, neither artificial viscosity nor second order interpolation of the electric current in the constrained transport seems to help. It should also be mentioned that the velocities at the same height level (not shown here) look less wiggly and show less grid structure than the temperature does.

Electric current denity

We can see a similar behaviour in the electric current density. Figure 7 shows a vertical cross section of the logarithm of the absolute electric current density from a simulation with HLL Van Leer (top) and from a simulation with HLL PP (bottom). The solution in the bottom panel is not as shaky as the temperature plot in Figure 4 (bottom) but the numerical grid is clearly visible. Figure 8 shows the logarithm of the absolute electric current density from a simulation with HLL PP *and* `c_visartificial=1.0` (top) and with `N_orderConstrainedTransport=2` (bottom). Again, neither artificial viscosity nor second order interpolation of the electric current in the constrained transport make a big difference to the original solution in Figure 7 (bottom).

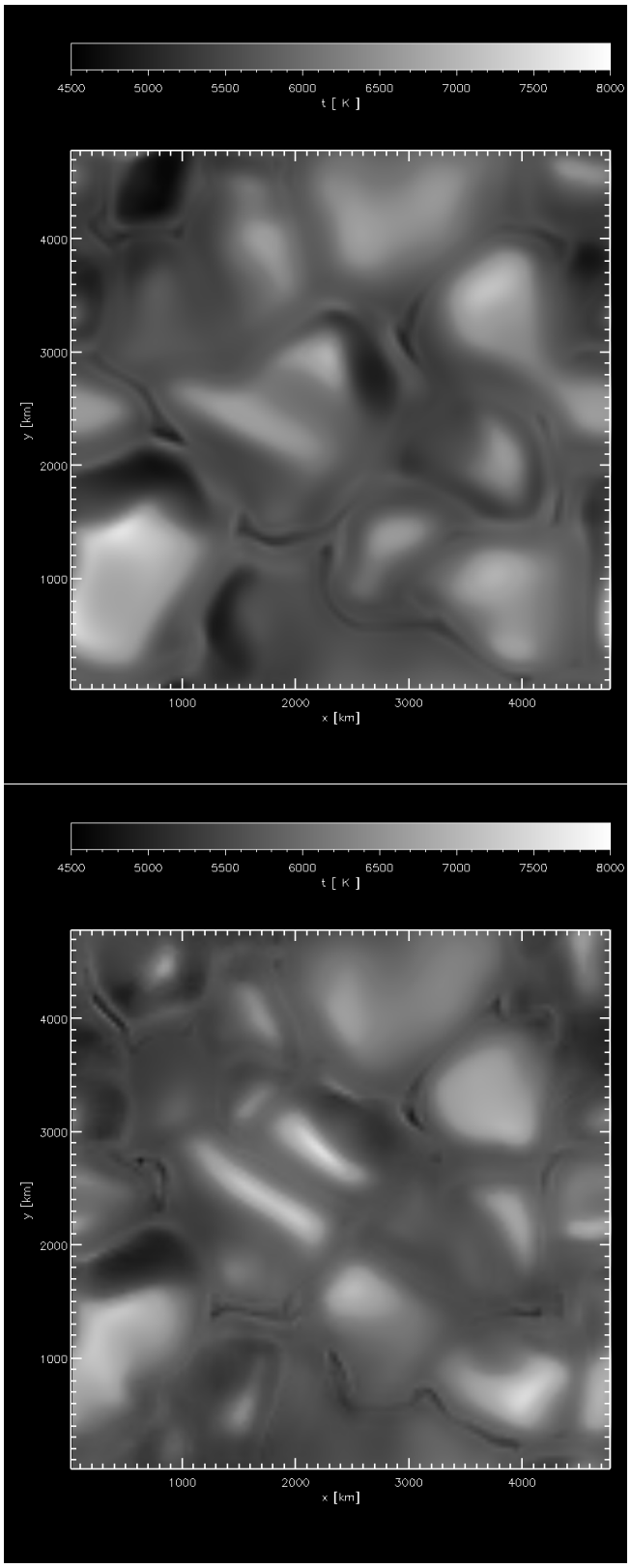

Figure 3: Temperature at a level of $\langle\tau\rangle = 1$ for the simulation with HLL and Van Leer (top panel) and the simulation with HLL and PP (bottom panel).

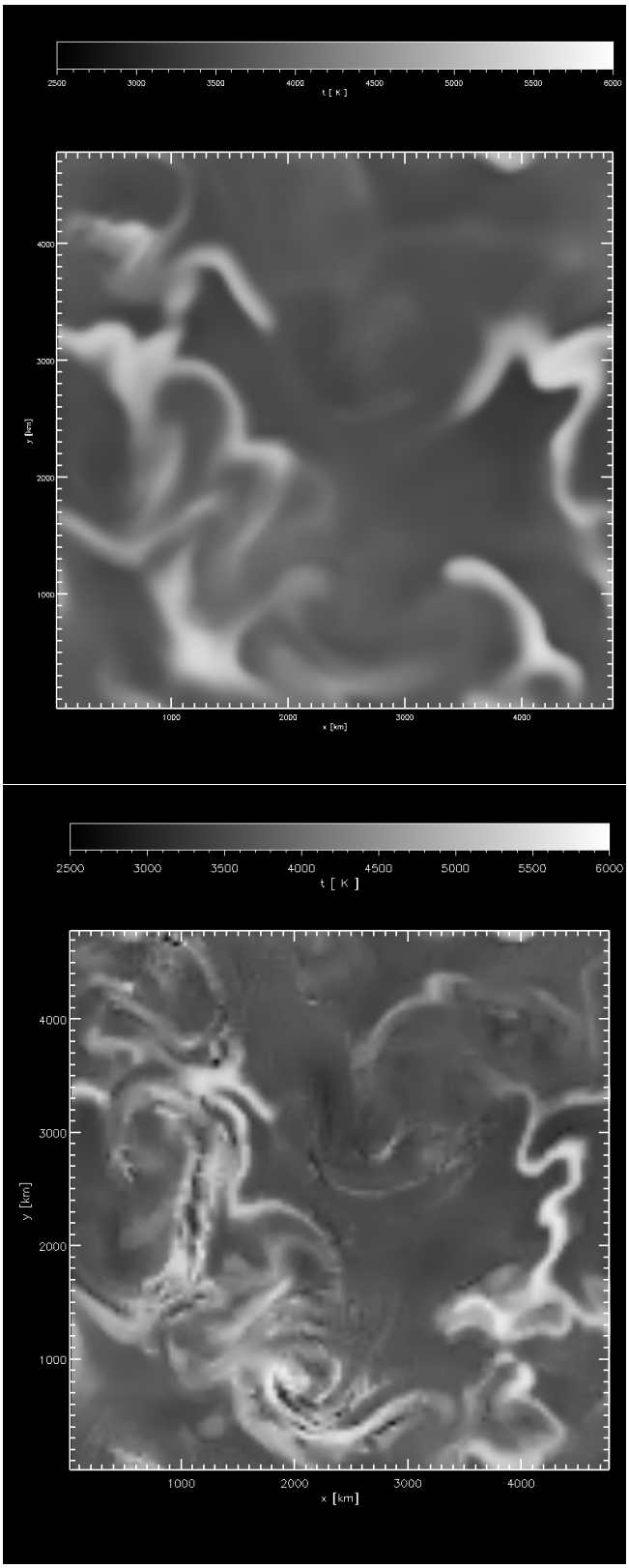

Figure 4: Temperature at a level of 1200 km above $\langle \tau \rangle = 1$ for the simulation with HLL and Van Leer (top panel) and the simulation with HLL and PP (bottom panel).

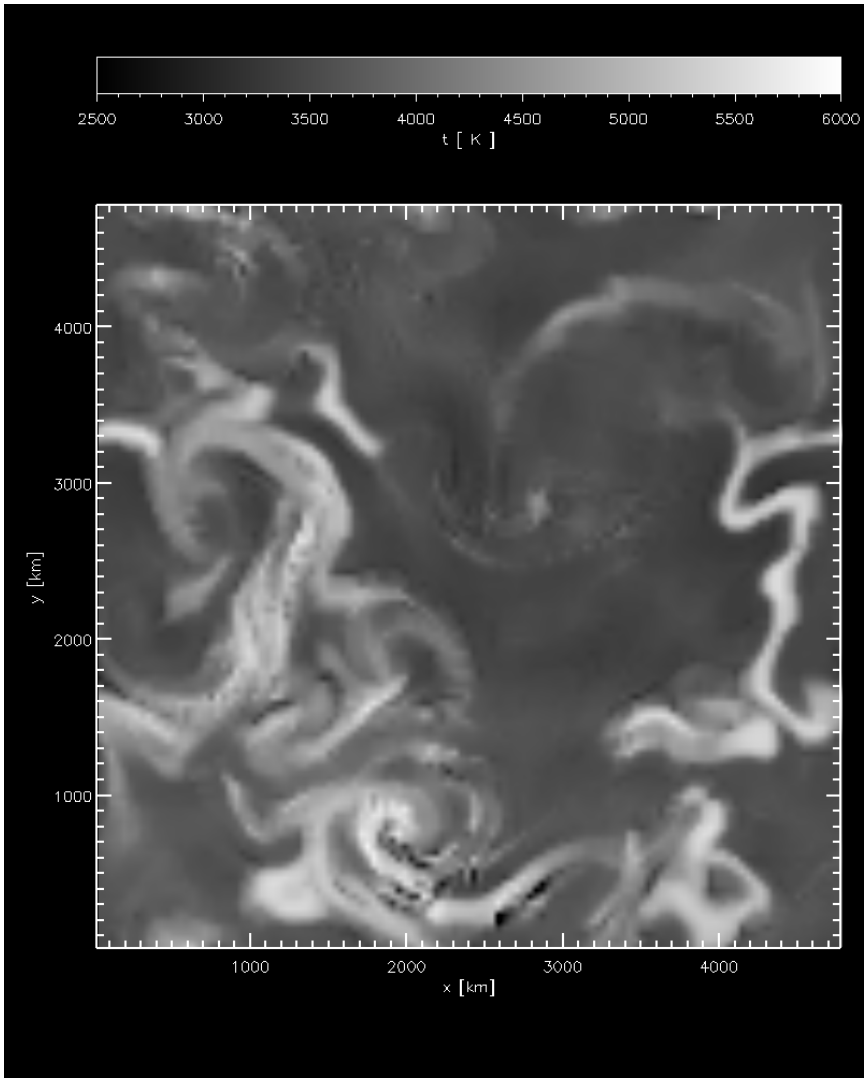

Figure 5: Temperature at a level of 1200 km above $\langle\tau\rangle = 1$ for the simulation with HLL and PP *and* c_visartificial=1.0.

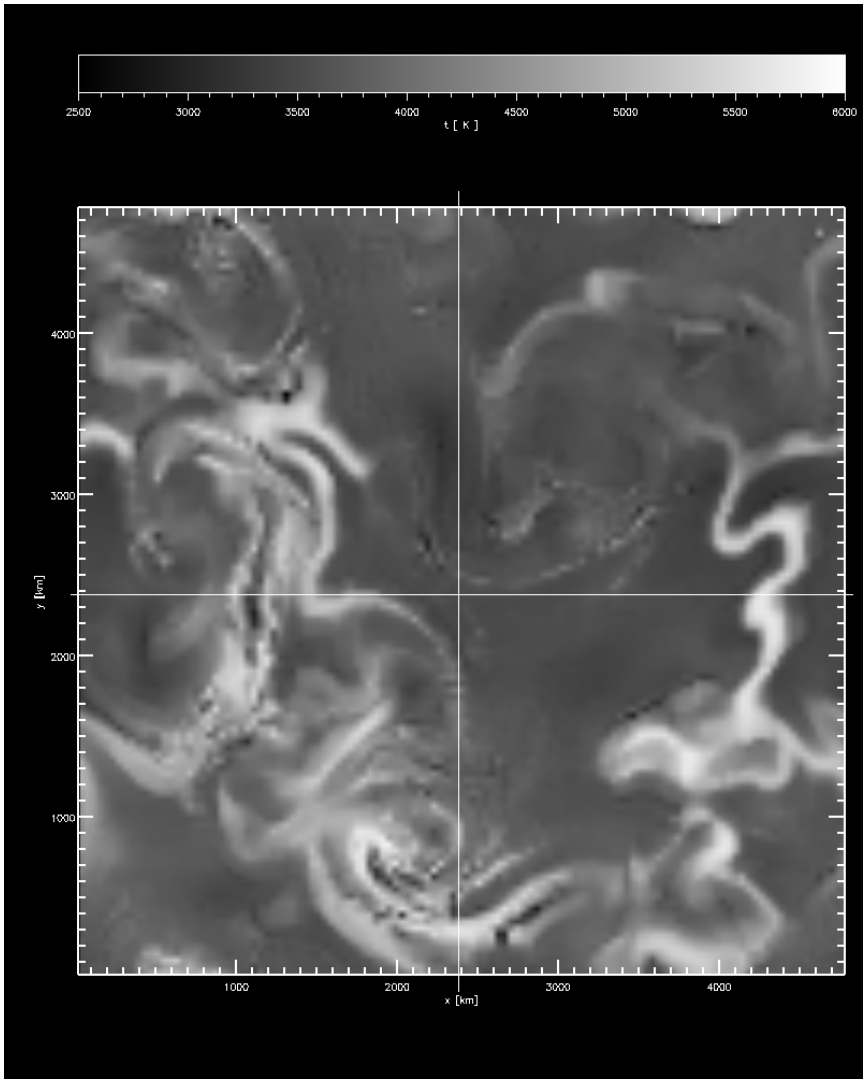

Figure 6: Temperature at a level of 1200 km above $\langle\tau\rangle = 1$ for the simulation with HLL and PP *and* N_orderConstrainedTransport=2.

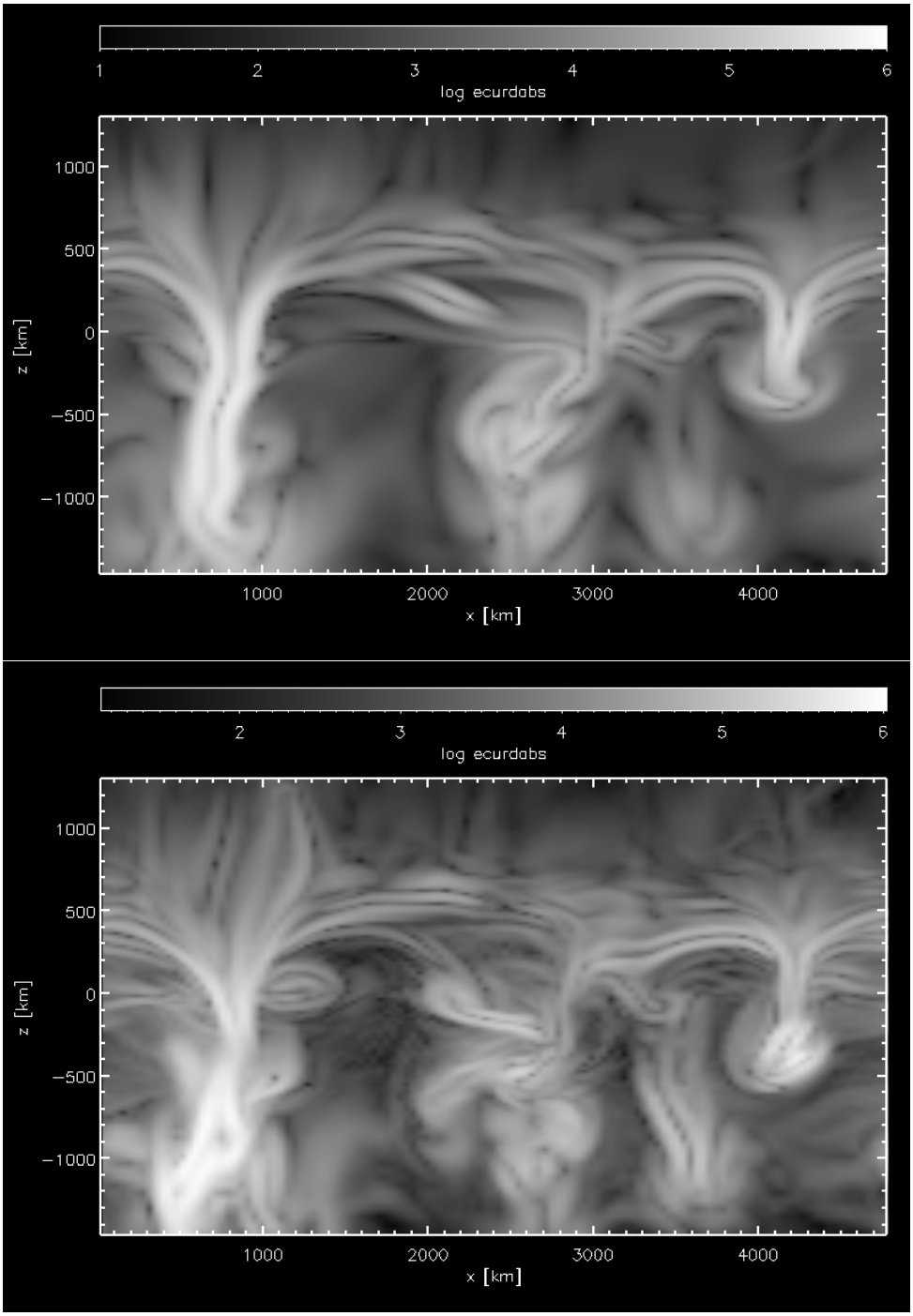

Figure 7: Logarithm of the absolute electric current density in a vertical cross section at $y = 2380$ km. Top: HLL Van Leer. Bottom: HLL PP.

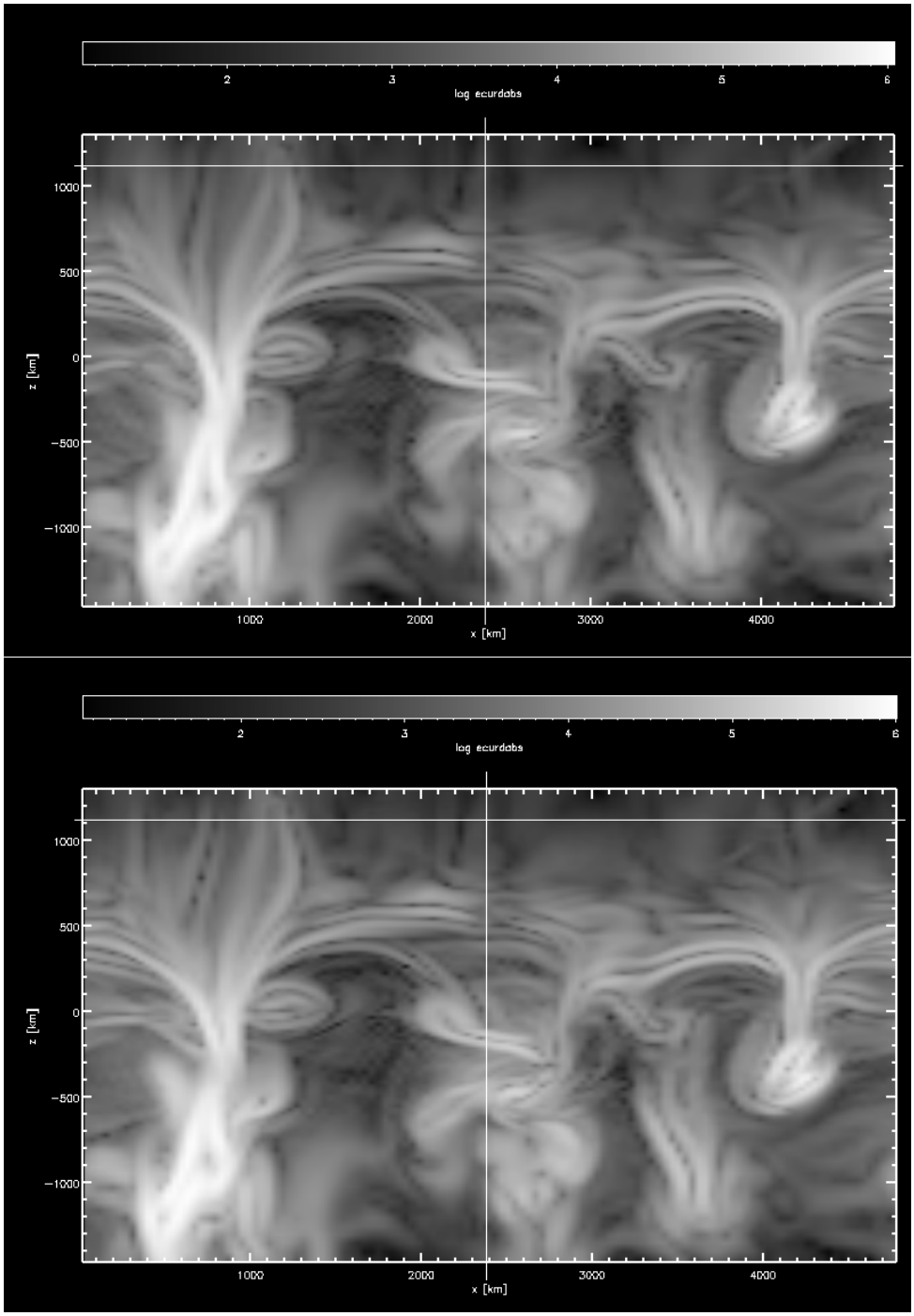

Figure 8: Logarithm of the absolute electric current density in a vertical cross section at $y = 2380$ km. Simulation with HLL PP. Top: c_visartificial=1.0. Bottom: N_orderConstrainedTransport=2.

Simulation with $B = 0$

We have also carried out a simulation with either setting the initial magnetic field to zero or omitting the magnetic field all together depending on wether computing with HLLMHD or Roe, respectively. We did this with a four times larger box, starting from relaxed thermal convection. Figure 9 shows the temperature at a height of 1200 km above $\langle\tau\rangle = 1$ after 540 s when computing with HLLMHD and Van Leer reconstruction. Figure 10 shows the same quantiy when computing with HLLMHD and PP reconstruction. Figure 11 shows the solution with the Roe solver and Van Leer reconstruction. Surprisingly, this time all the solutions look quite similar. HLL PP does hardly show more grid structure than the Roe solver does. The pattern in the two solutions match closely, while that of HLL Van Leer deviates more.

Fig. 12 shows the emergent bolometric intensity from the three models with vanishing magnetic field. We see that the HLL solver with PP reconstruction comes close to the solution with the Roe solver.

Conclusion

Generally, HLL with PP reconstruction produces more fine structure and details in all quantities compared to HLL with Van Leer reconstruction. When setting the magnetic field to zero, we find that the solution with HLL and PP closely matches the solution from the Roe solver with Van Leer reconstruction, while the corresponding solution with HLL and Van Leer markedly deviates after 540 s and details are strongly diffused. The only problem with HLL and PP is that the temperature (and internal energy and derived quantities) in chromospheric heights show strong wiggles and saw-teeth. The numerical grid is clearly visible. Interestingly, this problem is absent when advancing a solution with $B = 0$.

The fact that the problem is worst in the temperature points to the energy equation and the problem of computing $p_{\rm gas}$ from $e_{\rm tot}$. We have therefore made a test run with using the internal energy equation exclusively (by setting `beta_inv`=0.0) however without sweeping success although the solution is markedly smoother. Likewise, increasing the artificial viscosity or setting the order of interpolation of the electric currents to two does not help.

We plan to do some more tests like a simulation with a finite electric conductivity and one with double precision. I wonder if the compiler macro `rhd_roe1d_slope_l01` may have an effect on HLL PP? In principle, what we observe is that PP alone is a bit too aggressive and therefore, mixing with MinMod might help to produce a smoother solution. However, the manual says that this parameter was not recognized by HLLMHD. Some hybrid of PP with Van Leer (possibly in dependence of β-plasma) would possibly help. For a brut force approach one could post factum advance each individual snapshot of a simulation run with Van Leer for a few time steps in order to obtain smooth solutions without sacrifying accuracy.

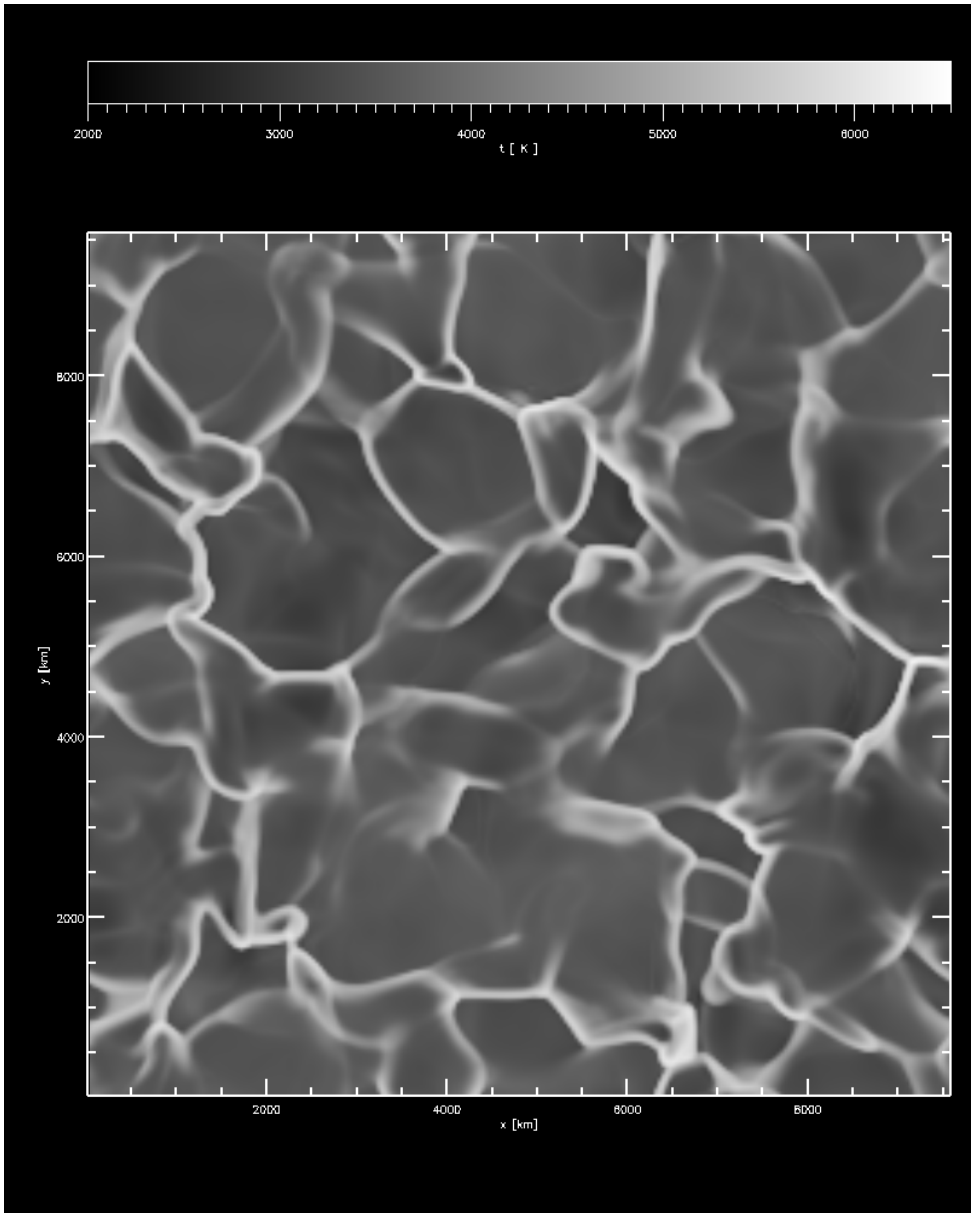

Figure 9: Temperature at a level of 1200 km above $\langle\tau\rangle = 1$ for the simulation with HLL and van Leer reconstruction. The magnetic field is $B = 0$.

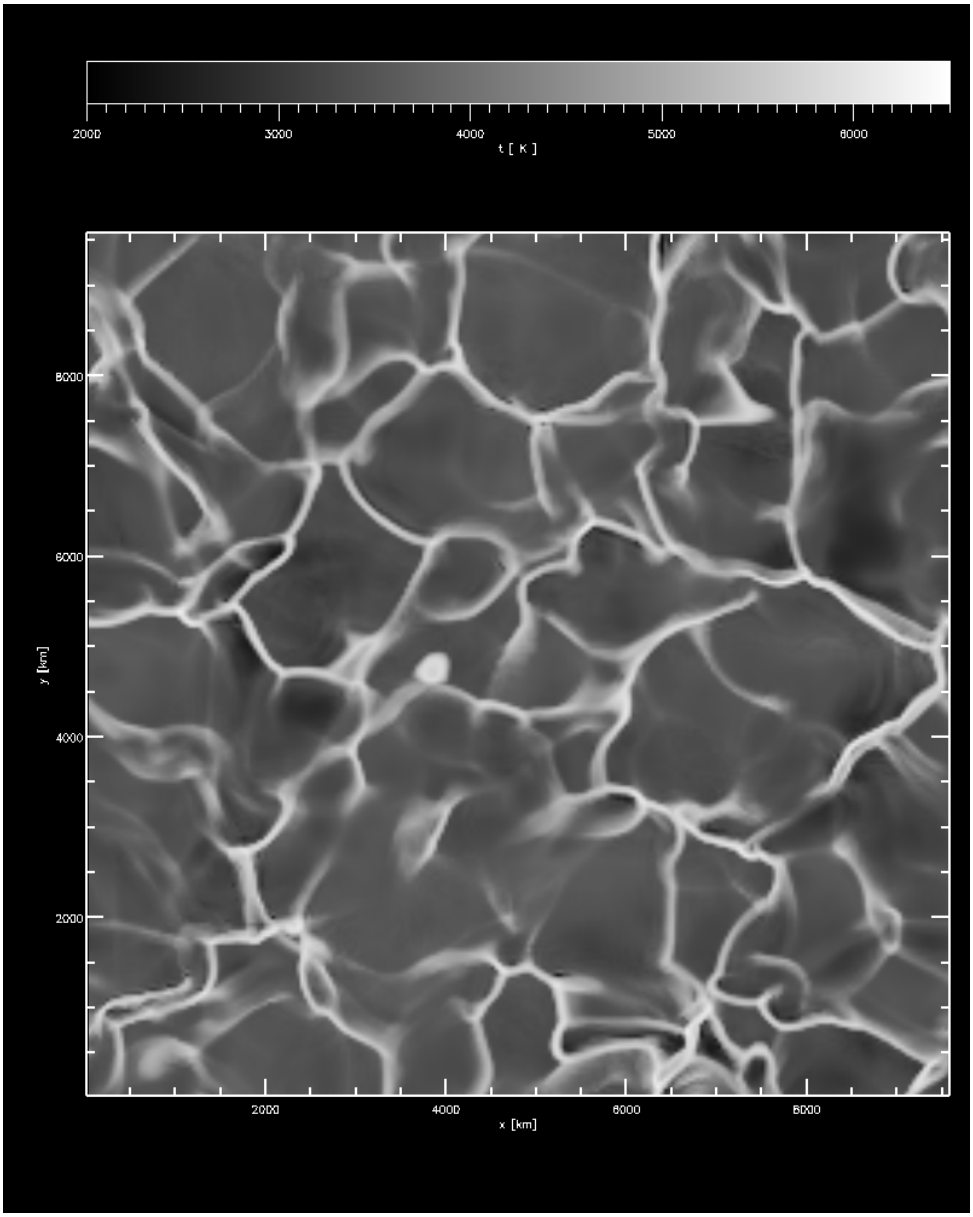

Figure 10: Temperature at a level of 1200 km above $\langle \tau \rangle = 1$ for the simulation with HLL and PP reconstruction. The magnetic field is $B = 0$.

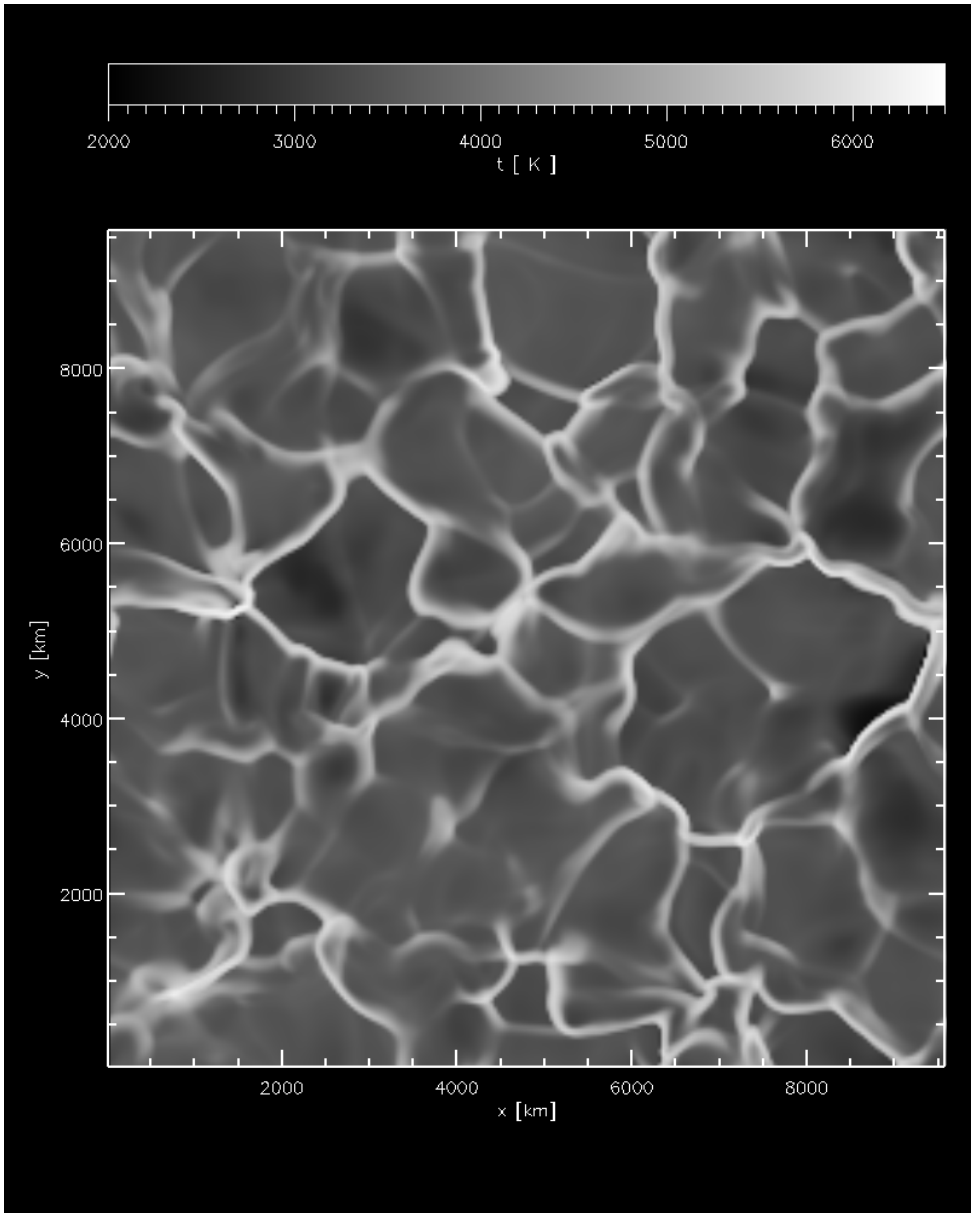

Figure 11: Temperature at a level of 1200 km above $\langle\tau\rangle = 1$ for the simulation with Roe and Van Leer reconstruction. There is no magnetic field present.

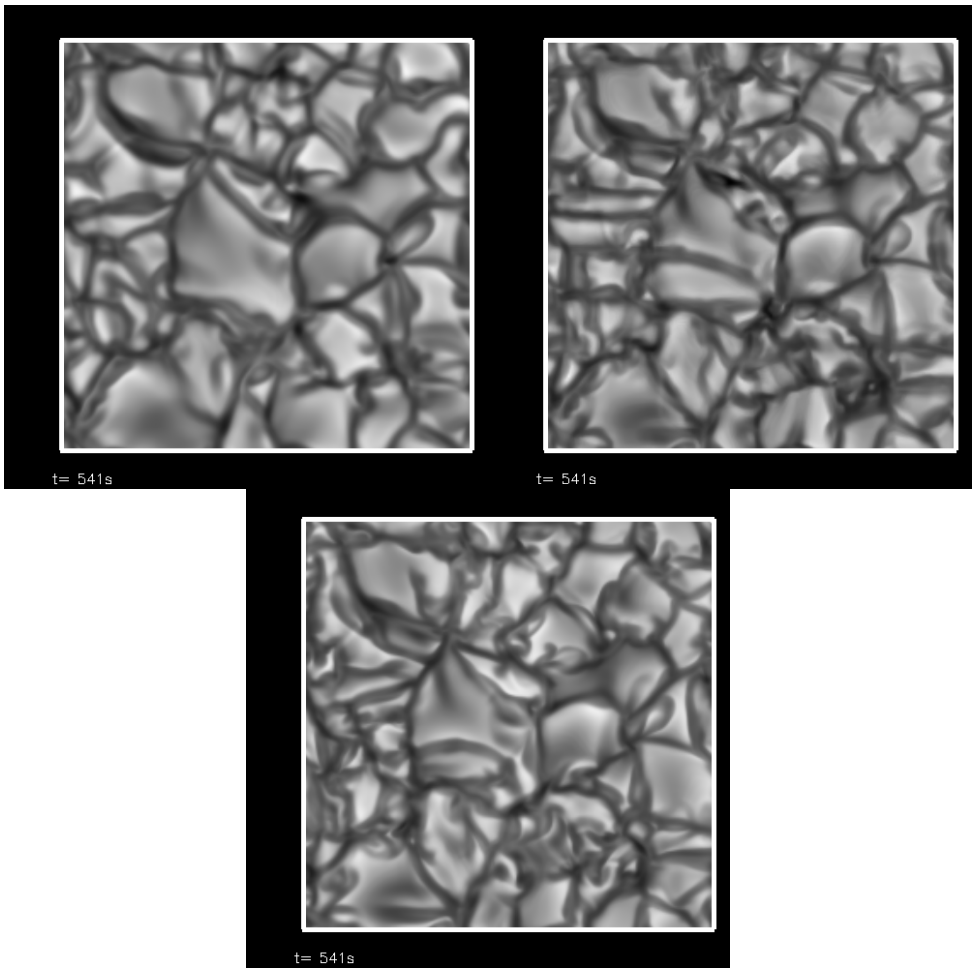

Figure 12: Bolometric intensity from a model advanced for 540 s with HLLMHD and Van Leer reconstruction (top left panel), HLLMHD and PP reconstruction (top right panel), and with the Roe solver and Van Leer reconstruction (bottom panel).